











TECH BRIEFS

NATIONAL AERONAUTICS AND SPACE ADMINISTRATION

-  **Technology Focus**
-  **Electronics/Computers**
-  **Software**
-  **Materials**
-  **Mechanics/Machinery**
-  **Manufacturing**
-  **Bio-Medical**
-  **Physical Sciences**
-  **Information Sciences**
-  **Books and Reports**

INTRODUCTION

Tech Briefs are short announcements of innovations originating from research and development activities of the National Aeronautics and Space Administration. They emphasize information considered likely to be transferable across industrial, regional, or disciplinary lines and are issued to encourage commercial application.

Additional Information on NASA Tech Briefs and TSPs

Additional information announced herein may be obtained from the NASA Technical Reports Server: <http://ntrs.nasa.gov>.

Please reference the control numbers appearing at the end of each Tech Brief. Information on NASA's Innovative Partnerships Program (IPP), its documents, and services is available on the World Wide Web at <http://www.ipp.nasa.gov>.

Innovative Partnerships Offices are located at NASA field centers to provide technology-transfer access to industrial users. Inquiries can be made by contacting NASA field centers listed below.

NASA Field Centers and Program Offices

Ames Research Center

David Morse
(650) 604-4724
david.r.morse@nasa.gov

Dryden Flight Research Center

Ron Young
(661) 276-3741
ronald.m.young@nasa.gov

Glenn Research Center

Kimberly A. Dalgleish-Miller
(216) 433-8047
kimberly.a.dalgleish@nasa.gov

Goddard Space Flight Center

Nona Cheeks
(301) 286-5810
nona.k.cheeks@nasa.gov

Jet Propulsion Laboratory

Dan Broderick
(818) 354-1314
daniel.f.broderick@jpl.nasa.gov

Johnson Space Center

John E. James
(281) 483-3809
john.e.james@nasa.gov

Kennedy Space Center

David R. Makufka
(321) 867-6227
david.r.makufka@nasa.gov

Langley Research Center

Michelle Ferebee
(757) 864-5617
michelle.t.ferebee@nasa.gov

Marshall Space Flight Center

Terry L. Taylor
(256) 544-5916
terry.taylor@nasa.gov

Stennis Space Center

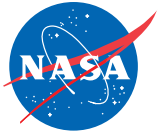
Ramona Travis
(228) 688-3832
ramona.e.travis@ssc.nasa.gov

NASA Headquarters

Daniel Lockney,
Technology Transfer Program Executive
(202) 358-2037
daniel.p.lockney@nasa.gov

Small Business Innovation Research (SBIR) & Small Business Technology Transfer (STTR) Programs

Rich Leshner, Program Executive
(202) 358-4920
rleshner@nasa.gov



TECH BRIEFS

NATIONAL AERONAUTICS AND SPACE ADMINISTRATION



- 5 Technology Focus: Sensors**
- 5 Multi-Source Autonomous Response for Targeting and Monitoring of Volcanic Activity
 - 6 Software Suite to Support In-Flight Characterization of Remote Sensing Systems
 - 6 Visual Image Sensor Organ Replacement



- 7 Electronics/Computers**
- 7 Ultra-Wideband, Dual-Polarized, Beam-Steering P-Band Array Antenna
 - 7 Centering a DDR Strobe in the Middle of a Data Packet
 - 8 Using a Commercial Ethernet PHY Device in a Radiation Environment
 - 8 Submerged AUV Charging Station



- 11 Mechanics/Machinery**
- 11 Habitat Demonstration Unit (HDU) Vertical Cylinder Habitat
 - 12 Origami-Inspired Folding of Thick, Rigid Panels



- 13 Bio-Medical**
- 13 A Novel Protocol for Decoating and Permeabilizing Bacterial Spores for Epifluorescent Microscopy
 - 13 Method and Apparatus for Automated Isolation of Nucleic Acids from Small Cell Samples
 - 14 Enabling Microliquid Chromatography by Microbead Packing of Microchannels
 - 14 On-Command Force and Torque Impeding Devices (OC-FTID) Using ERF



- 17 Physical Sciences**
- 17 Deployable Fresnel Rings
 - 18 Transition-Edge Hot-Electron Microbolometers for Millimeter and Submillimeter Astrophysics



- 19 Software**
- 19 Spacecraft Trajectory Analysis and Mission Planning Simulation (STAMPS) Software
 - 19 Cross Support Transfer Service (CSTS) Framework Library
 - 19 Arbitrary Shape Deformation in CFD Design
 - 19 Range Safety Flight Elevation Limit Calculation Software



- 21 Information Technologies**
- 21 Frequency-Modulated, Continuous-Wave Laser Ranging Using Photon-Counting Detectors
 - 21 Calculation of Operations Efficiency Factors for Mars Surface Missions
 - 22 GPU Lossless Hyperspectral Data Compression System
 - 22 Robust, Optimal Subsonic Airfoil Shapes
 - 23 Protograph-Based Raptor-Like Codes
 - 23 Fuzzy Neuron: Method and Hardware Realization
 - 24 Kalman Filter Input Processor for Boresight Calibration
 - 24 Organizing Compression of Hyperspectral Imagery to Allow Efficient Parallel Decompression
 - 25 Temperature Dependences of Mechanisms Responsible for the Water-Vapor Continuum Absorption

This document was prepared under the sponsorship of the National Aeronautics and Space Administration. Neither the United States Government nor any person acting on behalf of the United States Government assumes any liability resulting from the use of the information contained in this document, or warrants that such use will be free from privately owned rights.



Multi-Source Autonomous Response for Targeting and Monitoring of Volcanic Activity

This concept has great relevance to Earth science and future planetary exploration.

NASA's Jet Propulsion Laboratory, Pasadena, California

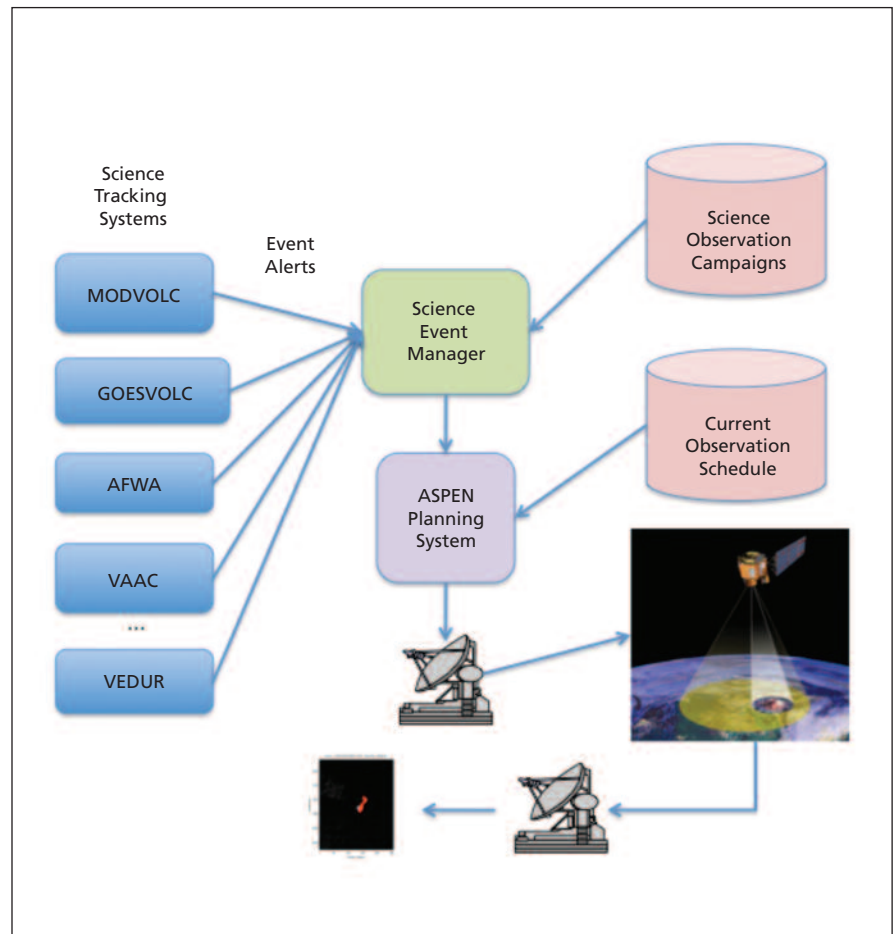
The study of volcanoes is important for both purely scientific and human survival reasons. From a scientific standpoint, volcanic gas and ash emissions contribute significantly to the terrestrial atmosphere. Ash depositions and lava flows can also greatly affect local environments. From a human survival standpoint, many people live within the reach of active volcanoes, and therefore can be endangered by both atmospheric (ash, debris) toxicity and lava flow.

There are many potential information sources that can be used to determine how to best monitor volcanic activity worldwide. These are of varying temporal frequency, spatial regard, method of access, and reliability. The problem is how to incorporate all of these inputs in a general framework to assign/task/reconfigure assets to monitor events in a timely fashion.

In situ sensing can provide a valuable range of complementary information such as seismographic, discharge, acoustic, and other data. However, many volcanoes are not instrumented with *in situ* sensors, and those that have sensor networks are restricted to a relatively small numbers of point sensors. Consequently, ideal volcanic study synergistically combines space and *in situ* measurements.

This work demonstrates an effort to integrate spaceborne sensing from MODIS (Terra and Aqua), ALI (EO-1), Worldview-2, and *in situ* sensing in an automated scheme to improve global volcano monitoring. Specifically, it is a "sensor web" concept in which a number of volcano monitoring systems are linked together to monitor volcanic activity more accurately, and this activity measurement automatically tasks space assets to acquire further satellite imagery of ongoing volcanic activity.

A general framework was developed for evidence combination that accounts for multiple information sources in a scientist-directed fashion to weigh inputs and allocate observations based on



The dataflow of the **Sensor Web System** uses alert systems to task volcano observations automatically based on scientist-specified observation campaigns.

the confidence of an events occurrence, rarity of the event at that location, and other scientists' inputs. The software framework uses multiple source languages and is a general framework for combining inputs and incrementally submitting observation requests/reconfigurations, accounting for prior requests.

The autonomous aspect of operations is unique, especially in the context of the wide range of inputs that includes manually inputted electronic reports (such as the Air Force Weather

Advisories), automated satellite-based detection methods (such as MODVOLC and GOESVOLC), and *in situ* sensor networks.

This work was done by Ashley G. Davies, Joshua R. Doubleday, and Daniel Q. Tran of Caltech for NASA's Jet Propulsion Laboratory. EO-1 is managed by Goddard Space Flight Center. Further information is contained in a TSP (see page 1).

The software used in this innovation is available for commercial licensing. Please contact Dan Broderick at Daniel.F.Broderick@jpl.nasa.gov. Refer to NPO-48148.

Software Suite to Support In-Flight Characterization of Remote Sensing Systems

Stennis Space Center, Mississippi

A characterization software suite was developed to facilitate NASA's in-flight characterization of commercial remote sensing systems. Characterization of aerial and satellite systems requires knowledge of ground characteristics, or ground truth. This information is typically obtained with instruments taking measurements prior to or during a remote sensing system overpass. Acquired ground-truth data, which can consist of hundreds of measurements with different data formats, must be processed before it can be used in the characterization. Accurate in-flight characterization of remote sensing systems relies on multiple field data acquisitions that are efficiently processed, with minimal error.

To address the need for timely, reproducible ground-truth data, a characterization software suite was developed to automate the data processing methods. The characterization software suite is engineering code, requiring some prior

knowledge and expertise to run. The suite consists of component scripts for each of the three main in-flight characterization types: radiometric, geometric, and spatial. The component scripts for the radiometric characterization operate primarily by reading the raw data acquired by the field instruments, combining it with other applicable information, and then reducing it to a format that is appropriate for input into MODTRAN (MODerate resolution atmospheric TRANsmission), an Air Force Research Laboratory-developed radiative transport code used to predict at-sensor measurements. The geometric scripts operate by comparing identified target locations from the remote sensing image to known target locations, producing circular error statistics defined by the Federal Geographic Data Committee Standards. The spatial scripts analyze a target edge within the image, and produce estimates of Rel-

ative Edge Response and the value of the Modulation Transfer Function at the Nyquist frequency.

The software suite enables rapid, efficient, automated processing of ground-truth data, which has been used to provide reproducible characterizations on a number of commercial remote sensing systems. Overall, this characterization software suite improves the reliability of ground-truth data processing techniques that are required for remote sensing system in-flight characterizations.

This work was done by Thomas Stanley of Stennis Space Center; Robert Ryan, Mary Pagnutti, Slawomir Blonski, Kenton Ross, Kara Holekamp, Gerald Gasser, and Wes Tabor of Lockheed Martin; and Ronald Vaughan of CSC.

For more information, contact the SSC Office of Center Chief Technologist at 228-688-1929 or by email at SSC-Technology@nasa.gov. Refer to SSC-00393.

Visual Image Sensor Organ Replacement

Ames Research Center, Moffett Field, California

This innovation is a system that augments human vision through a technique called "Sensing Super-position" using a Visual Instrument Sensory Organ Replacement (VISOR) device. The VISOR device translates visual and other sensors (i.e., thermal) into sounds to enable very difficult sensing tasks.

Three-dimensional spatial brightness and multi-spectral maps of a sensed image are processed using real-time image processing techniques (e.g. histogram normalization) and transformed into a two-dimensional map of an audio

signal as a function of frequency and time. Because the human hearing system is capable of learning to process and interpret extremely complicated and rapidly changing auditory patterns, the translation of images into sounds reduces the risk of accidentally filtering out important clues.

The VISOR device was developed to augment the current state-of-the-art head-mounted (helmet) display systems. It provides the ability to sense beyond the human visible light range, to increase human sensing resolution, to use

wider angle visual perception, and to improve the ability to sense distances. It also allows compensation for movement by the human or changes in the scene being viewed.

This work was done by David A. Maluf of Ames Research Center. Further information is contained in a TSP (see page 1).

Inquiries concerning rights for the commercial use of this invention should be addressed to the Ames Technology Partnerships Division at 1-855-NASA-BIZ (1-855-6272-249) or sumedha.garud@nasa.gov. Refer to ARC-15578-2.



Ultra-Wideband, Dual-Polarized, Beam-Steering P-Band Array Antenna

The novel design geometry can be scaled with minor modifications.

Goddard Space Flight Center, Greenbelt, Maryland

A dual-polarized, wide-bandwidth (200 MHz for one polarization, 100 MHz for the orthogonal polarization) antenna array at P-band was designed to be driven by NASA's EcoSAR digital beam former. EcoSAR requires two wide P-band antenna arrays mounted on the wings of an aircraft, each capable of steering its main beam up to 35° off-boresight, allowing the twin radar beams to be steered at angles to the flight path. The science requirements are mainly for dual-polarization capability and a wide bandwidth of operation of up to 200 MHz if possible, but at least 100 MHz with high polarization port isolation and low cross-polarization. The novel design geometry can be scaled with minor modifications up to about four times higher or down to about half the current design frequencies for any application requiring a dual-polarized, wide-bandwidth steerable antenna array.

EcoSAR is an airborne interferometric P-band synthetic aperture radar (SAR) research application for studying two- and three-dimensional fine-scale measurements of terrestrial ecosystem structure and biomass, which will ulti-

mately aid in the broader study of the carbon cycle and climate change. The two 2×8 element P-band antenna arrays required by the system will be separated by a baseline of about 25 m, allowing for interferometry measurements. The wide 100-to-200-MHz bandwidth dual-polarized beams employed will allow the determination of the amount of biomass and even tree height on the ground.

To reduce the size of the patches along the boresight dimension in order to fit them into the available space, two techniques were employed. One technique is to add slots along the edges of each patch where the main electric currents are expected to flow, and the other technique is to bend the central part of the patch away from the ground plane. The latter also facilitates higher mechanical rigidity.

The high port isolation of more than 40 dB was achieved by employing a highly symmetrical feed mechanism for each pair of elements: three apertures coupling to the patch elements were placed along the two symmetry lines of the antenna element pair. Two apertures were used in tandem to excite two

of the stacked patch elements for one polarization; the other was used to excite one element from one side and the other element from the other side, opposite in phase, taking care of the remaining polarization. The apertures narrow down to a small gap where they are excited by a crossing microstrip line to prevent any asymmetrical excitation of the two sides of the aperture gap, minimizing port-to-port coupling.

Using patches that are non-planar leads to higher mechanical rigidity and smaller patch sizes to fit into the available space. Aperture coupling minimizes direct metal-to-metal connections. Using an aperture coupling feed mechanism results in a feed network for two antenna elements with a total of three feed points, plus one simple in-phase combiner to reduce it to two ports. It greatly reduces the complexity of the alternative, but more conventional, way of feeding a pair of two dual-polarized elements with high port isolation.

This work was done by Cornelis du Toit of DSFG for Goddard Space Flight Center. Further information is contained in a TSP (see page 1). GSC-16778-1

Centering a DDR Strobe in the Middle of a Data Packet

Lyndon B. Johnson Space Center, Houston, Texas

The Orion CEV Northstar ASIC (application-specific integrated circuit) project required a DDR (double data rate) memory bus driver/receiver (DDR PHY block) to interface with external DDR memory. The DDR interface (JESD79C) is based on a source synchronous strobe (DQS) that is sent along with each packet of data (DQ). New data is provided concurrently with each edge of strobe and is sent irregularly. In order to capture this data, the strobe needs to be delayed and used to latch the data into a register.

A circuit solves the need for training a DDR PRY block by incorporating a PVT-compensated delay element in the strobe path. This circuit takes an external reference clock signal and uses the regular clock to calibrate a known delay through a data path. The compensated delay DQS signal is then used to capture the DQ data in a normal register. This register structure can be configured as a FIFO (first in first out), in order to transfer data from the DDR domain to the system clock domain. This design is different in that it does

not rely upon the need for training the system response, nor does it use a PLL (phase locked loop) or a DLL (delay locked loop) to provide an offset of the strobe signal.

The circuit is created using standard ASIC building blocks, plus the PVT (process, voltage, and temperature) compensated delay line. The design uses a globally available system clock as a reference, alleviating the need to operate synchronously with the remote memory. The reference clock conditions the PVT compensated delay line to provide a pre-

determined amount of delay to any data signal that passes through this delay line. The delay line is programmed in degrees of offset, so that one could think of the clock period representing 360° of delay. In an ideal environment, delaying the strobe 1/4 of a clock cycle (90°) would place the strobe in the middle of the data packet. This delayed strobe can then be used to clock the data into a reg-

ister, satisfying setup and hold requirements of the system.

This work was done by Michael Johnson, Dave Nelson, James Seefeldt, Weston Roper, and Craig Passow of Honeywell for Johnson Space Center. For further information, contact the JSC Innovation Partnerships Office at (281) 483-3809.

Title to this invention has been waived under the provisions of the National Aero-

navics and Space Act {42 U.S.C. 2457(f)}, to Honeywell. Inquiries concerning licenses for its commercial development should be addressed to:

*Honeywell
P.O. Box 52199
Phoenix, AZ 85072-2199*

Refer to MSC-24931-1, volume and number of this NASA Tech Briefs issue, and the page number.

Using a Commercial Ethernet PHY Device in a Radiation Environment

Lyndon B. Johnson Space Center, Houston, Texas

This work involved placing a commercial Ethernet PHY on its own power boundary, with limited current supply, and providing detection methods to determine when the device is not operating and when it needs either a reset or power-cycle. The device must be radiation-tested and free of destructive latch-up errors.

The commercial Ethernet PHY's own power boundary must be supplied by a current-limited power regulator that must have an enable (for power cycling), and its maximum power output must not exceed the PHY's input requirements, thus preventing damage to the device. A regulator with configurable output limits and short-circuit protection (such as the RHFL4913, rad-

hard positive voltage regulator family) is ideal. This will prevent a catastrophic failure due to radiation (such as a short between the commercial device's power and ground) from taking down the board's main power.

Logic provided on the board will detect errors in the PHY. An FPGA (field-programmable gate array) with embedded Ethernet MAC (Media Access Control) will work well. The error detection includes monitoring the PHY's interrupt line, and the status of the Ethernet's switched power. When the PHY is determined to be non-functional, the logic device resets the PHY, which will often clear radiation induced errors. If this doesn't work, the logic device power-cycles the FPGA by toggling the

regulator's enable input. This should clear almost all radiation induced errors provided the device is not latched up.

This work was done by Jeremy Parks, Michael Arani, and Roberto Arroyo of Honeywell Aerospace for Johnson Space Center. For further information, contact the JSC Innovation Partnerships Office at (281) 483-3809.

Title to this invention has been waived under the provisions of the National Aeronautics and Space Act {42 U.S.C. 2457(f)}, to Honeywell. Inquiries concerning licenses for its commercial development should be addressed to:

*Honeywell
P.O. Box 52199
Phoenix, AZ 85072-2199*

Refer to MSC-24934-1, volume and number of this NASA Tech Briefs issue, and the page number.

Submerged AUV Charging Station

Potential uses include studying ocean climate change, pollution, salinity, and currents.

NASA's Jet Propulsion Laboratory, Pasadena, California

Autonomous Underwater Vehicles (AUVs) are becoming increasingly important for military surveillance and mine detection. Most AUVs are battery powered and have limited lifetimes of a few days to a few weeks. This greatly limits the distance that AUVs can travel underwater. Using a series of submerged AUV charging stations, AUVs could travel a limited distance to the next charging station, recharge its batteries, and continue to the next charging station, thus traveling great distances in a relatively short time, similar to the Old West "Pony Express."

One solution is to use temperature differences at various depths in the

ocean to produce electricity, which is then stored in a submerged battery. It is preferred to have the upper buoy submerged a reasonable distance below the surface, so as not to be seen from above and not to be inadvertently destroyed by storms or ocean going vessels. In a previous invention, a phase change material (PCM) is melted (expanded) at warm temperatures, for example, 15 °C, and frozen (contracted) at cooler temperatures, for example, 8 °C.

Tubes containing the PCM, which could be paraffin such as pentadecane, would be inserted into a container filled with hydraulic oil. When the PCM is melted (expanded), it pushes the oil out

into a container that is pressurized to about 3,000 psi (≈20.7 MPa). When a valve is opened, the high-pressure oil passes through a hydraulic motor, which turns a generator and charges a battery. The low-pressure oil is finally reabsorbed into the PCM canister when the PCM tubes are frozen (contracted). Some of the electricity produced could be used to control an external bladder or a motor to the tether line, such that depth cycling is continued for a very long period of time.

Alternatively, after the electricity is generated by the hydraulic motor, the exiting low-pressure oil from the hydraulic motor could be vented directly

to an external bladder on the AUV, such that filling of the bladder causes the AUV to rise, and emptying of the bladder allows the AUV to descend. This type of direct buoyancy control is much more energy efficient than using electrical pumps in that the inefficiencies of converting thermal energy to electrical energy to mechanical energy is avoided.

AUV charging stations have been developed that use electricity produced by

waves on floating buoys and that use electricity from solar photovoltaics on floating buoys. This is the first device that has absolutely no floating or visible parts, and is thus impervious to storms, inadvertent ocean vessel collisions, or enemy sabotage.

This work was done by Jack A. Jones and Yi Chao of Caltech, and Thomas Curtin of NATP for NASA's Jet Propulsion Laboratory. Further information is contained in a TSP (see page 1).

In accordance with Public Law 96-517, the contractor has elected to retain title to this invention. Inquiries concerning rights for its commercial use should be addressed to:

*Innovative Technology Assets Management
JPL, Mail Stop 321-123*

*4800 Oak Grove Drive
Pasadena, CA 91109-8099*

E-mail: iaoffice@jpl.nasa.gov

Refer to NPO-46985, volume and number of this NASA Tech Briefs issue, and the page number.



Habitat Demonstration Unit (HDU) Vertical Cylinder Habitat

Modular habitats maximize floor area and are easy to join together.

Lyndon B. Johnson Space Center, Houston, Texas

NASA's Constellation Architecture Team defined an outpost scenario optimized for intensive mobility that uses small, highly mobile pressurized rovers supported by portable habitat modules that can be carried between locations of interest on the lunar surface. A compact vertical cylinder characterizes the habitat concept, where the large diameter maximizes usable flat floor area optimized for a gravity environment and allows for efficient internal layout. The module was sized to fit into payload fairings for the Constellation Ares V launch vehicle, and optimized for surface transport carried by the All-Terrain Hex-Limbed Extra-Terrestrial Explorer (ATHLETE) mobility system. Launch and other loads are carried through the barrel to a top and bottom truss that interfaces with a structural support unit (SSU). The SSU contains self-leveling feet and docking interfaces for Tri-ATHLETE grasping and heavy lift.

A pressurized module needed to be created that was appropriate for the lunar environment, could be easily re-

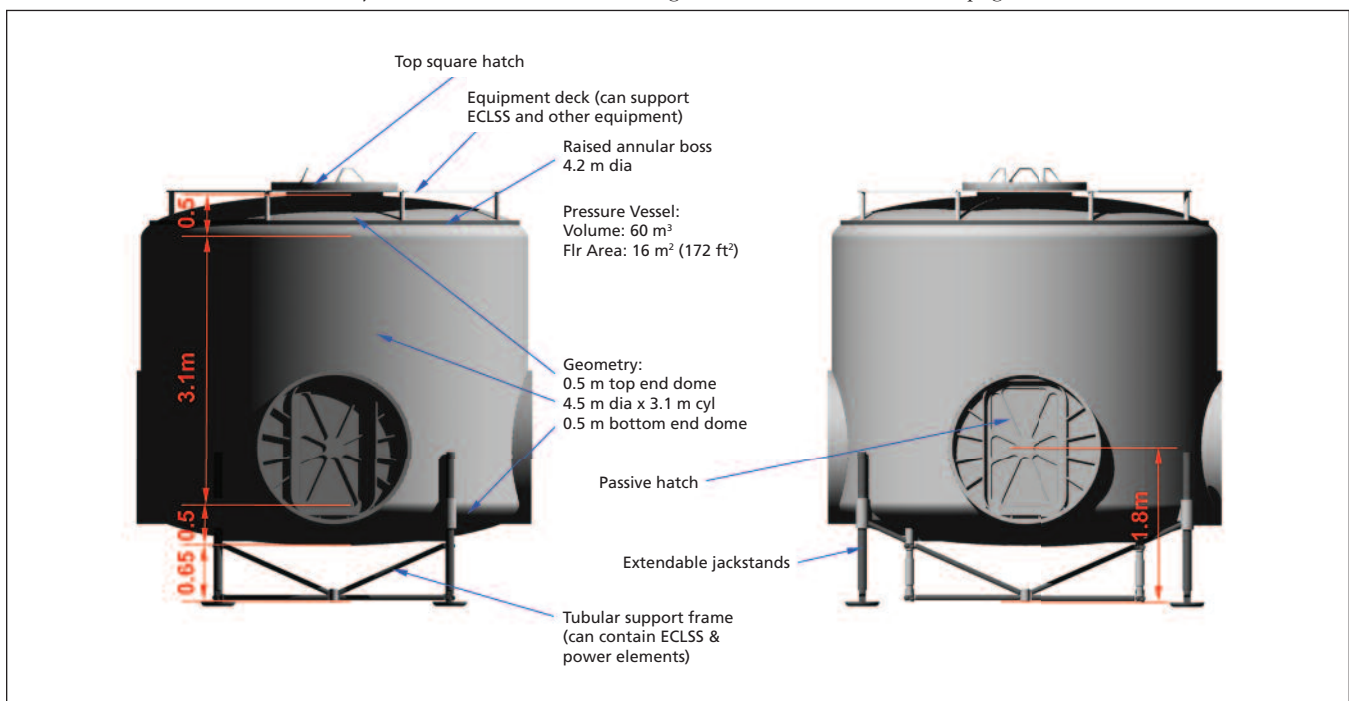
located to new locations, and could be docked together in multiples for expanding pressurized volume in a lunar outpost. It was determined that horizontally oriented pressure vessels did not optimize floor area, which takes advantage of the gravity vector for full use. Hybrid hard-inflatable habitats added an unproven degree of complexity that may eventually be worked out. Other versions of vertically oriented pressure vessels were either too big, bulky, or did not optimize floor area.

The purpose of the HDU vertical habitat module is to provide pressurized units that can be docked together in a modular way for lunar outpost pressurized volume expansion, and allow for other vehicles, rovers, and modules to be attached to the outpost to allow for IVA (intra-vehicular activity) transfer between them. The module is a vertically oriented cylinder with a large radius to allow for maximal floor area and use of volume. The modular, 5-m-diameter HDU vertical habitat module consists of a 2-m-high barrel with 0.6-m-

high end domes forming the 56-cubic-meter pressure vessel, and a 19-square-meter floor area. The module has up to four docking ports located orthogonally from each other around the perimeter, and up to one docking port each on the top or bottom end domes. In addition, the module has mounting trusses top and bottom for equipment, and to allow docking with the ATHLETE mobility system.

Novel or unique features of the HDU vertical habitat module include the node-like function with multiple pressure hatches for docking with other versions of itself and other modules and vehicles; the capacity to be carried by an ATHLETE mobility system; and the ability to attach inflatable 'attic' domes to the top for additional pressurized volume.

This work was done by Alan Howe, Kriss J. Kennedy, Tracy R. Gill, Terry O. Tri, Larry Toups, Robert I. Howard, Gary R. Spexarth, Stephen Cavanaugh, William M. Langford, and John T. Dorsey of Johnson Space Center. Further information is contained in a TSP (see page 1). MSC-25517-1



The Habitat Demonstration Unit (HDU) Vertical Cylinder Node features multiple pressure hatches for docking with other versions of itself and other modules and vehicles. (Note: ECLSS is Environmental Control and Life Support System.)

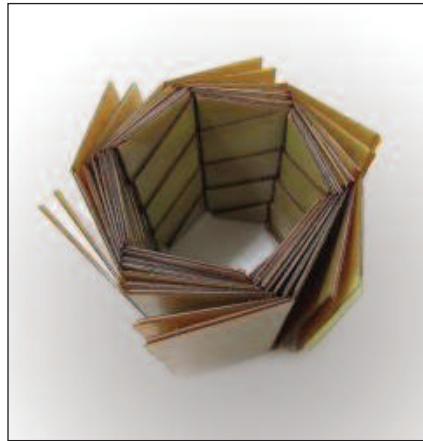
⚙️ Origami-Inspired Folding of Thick, Rigid Panels

Hinges are used to achieve the necessary folding.

NASA's Jet Propulsion Laboratory, Pasadena, California

To achieve power of 250 kW or greater, a large compression ratio of stowed-to-deployed area is needed. Origami folding patterns were used to inspire the folding of a solar array to achieve synchronous deployment; however, origami models are generally created for near-zero-thickness material. Panel thickness is one of the main challenges of origami-inspired design.

Three origami-inspired folding techniques (flasher, square twist, and map fold) were created with rigid panels and hinges. Hinge components are added to the model to enable folding of thick, rigid materials. Origami models are created assuming zero (or near zero) thickness. When a material with



A Membrane Backing enables the folding of a six-sided origami flasher with rigid panels.

finite thickness is used, the panels are required to bend around an increasingly thick fold as they move away from the center of the model. The two approaches for dealing with material thickness are to use membrane hinges to connect the panels, or to add panel hinges, or hinges of the same thickness, at an appropriate width to enable folding.

This work was done by Brian P. Trease, Mark W. Thomson, Deborah A. Sigel, and Phillip E. Walkemeyer of Caltech; Shannon Zirbel and Larry Howell of Brigham Young University; and Robert Lang of Lang Origami for NASA's Jet Propulsion Laboratory. Further information is contained in a TSP (see page 1). NPO-48861



A Novel Protocol for Decoating and Permeabilizing Bacterial Spores for Epifluorescent Microscopy

This technique can be used in semiconductor, pharmaceutical, and food processing industries.

NASA's Jet Propulsion Laboratory, Pasadena, California

Based on previously reported procedures for permeabilizing vegetative bacterial cells, and numerous trial-and-error attempts with bacterial endospores, a protocol was developed for effectively permeabilizing bacterial spores, which facilitated the applicability of fluorescent *in situ* hybridization (FISH) microscopy. Bacterial endospores were first purified from overgrown, sporulated suspensions of *B. pumilus* SAFR-032. Purified spores at a concentration of ≈ 10 million spores/mL then underwent proteinase-K treatment, in a solution of 468.5 μ L of 100 mM Tris-HCl, 30 μ L of 10% SDS, and 1.5 μ L of 20 mg/mL proteinase-K for ten minutes at 35 °C. Spores were then harvested by centrifugation (15,000 g for 15 minutes) and washed twice with sterile phosphate-buffered saline (PBS) solution. This washing process consisted of resuspending the spore pellets in 0.5 mL of PBS, vortexing momentarily, and harvesting again by centrifugation. Treated and washed spore pellets were then resuspended in 0.5 mL of decoating solution, which consisted of 4.8 g urea, 3 mL

Milli-Q water, 1 mL 0.5M Tris, 1 mL 1M dithiothreitol (DTT), and 2 mL 10% sodium-dodecylsulfate (SDS), and were incubated at 65 °C for 15 minutes while being shaken at 165 rpm.

Decoated spores were then, once again, washed twice with sterile PBS, and subjected to lysozyme/mutanolysin treatment (7 mg/mL lysozyme and 7U mutanolysin) for 15 minutes at 35 °C. Spores were again washed twice with sterile PBS, and spore pellets were resuspended in 1-mL of 2% SDS. This treatment, facilitating inner membrane permeabilization, lasted for ten minutes at room temperature. Permeabilized spores were washed two final times with PBS, and were resuspended in 200 μ L of sterile PBS. At this point, the spores were permeable and ready for downstream processing, such as oligonucleotide-probe infiltration, hybridization, and microscopic evaluation. FISH-microscopic imagery confirmed the effective and efficient ($\approx 50\%$ successful permeabilization and recovery) permeabilization of numerous spore preparations.

The novelty of the technology developed here is in its applicability to bacterial endospores. While protocols abound for the effective permeabilization of bacterial, archaeal, and eukaryotic vegetative cells, there are no such reliable methods for decoating and permeabilizing bacterial endospores in a manner that is amenable to downstream FISH microscopic analyses. This innovation enables the direct visualization and enumeration of spores via FISH-based microscopic techniques, circumventing the complications that accompany previously required germination regimes. The synergistic enzymatic weakening of the many spore layers facilitates a structural compromise that is just enough to render the spores permeable without degrading the spore to a level, which precludes it from recognition.

This work was done by Myron T. La Duc of Caltech, and Bidyut Mohapatra of the University of South Alabama for NASA's Jet Propulsion Laboratory. For more information, contact iaoffice@jpl.nasa.gov. NPO-48035

Method and Apparatus for Automated Isolation of Nucleic Acids from Small Cell Samples

Advantages include reduced or eliminated use of toxic reagents and operator-independent extraction.

Lyndon B. Johnson Space Center, Houston, Texas

RNA isolation is a ubiquitous need, driven by current emphasis on microarrays and miniaturization. With commercial systems requiring 100,000 to 1,000,000 cells for successful isolation, there is a growing need for a small-footprint, easy-to-use device that can harvest nucleic acids from much smaller cell samples (1,000 to 10,000 cells). The process of extraction of RNA from cell cultures is a complex, multi-step one, and requires timed, asynchronous operations with mul-

tiples reagents/buffers. An added complexity is the fragility of RNA (subject to degradation) and its reactivity to surface.

A novel, microfluidics-based, integrated cartridge has been developed that can fully automate the complex process of RNA isolation (lyse, capture, and elute RNA) from small cell culture samples. On-cartridge cell lysis is achieved using either reagents or high-strength electric fields made possible by the miniaturized format. Traditionally, silica-based,

porous-membrane formats have been used for RNA capture, requiring slow perfusion for effective capture. In this design, high efficiency capture/elution are achieved using a microsphere-based "microfluidized" format. Electrokinetic phenomena are harnessed to actively mix microspheres with the cell lysate and capture/elution buffer, providing important advantages in extraction efficiency, processing time, and operational flexibility. Successful RNA isolation was demon-

strated using both suspension (HL-60) and adherent (BHK-21) cells.

Novel features associated with this development are twofold. First, novel designs that execute needed processes with improved speed and efficiency were developed. These primarily encompass electric-field-driven lysis of cells. The configurations include electrode-containing constructs, or an “electrode-less” chip design, which is easy to fabricate and mitigates fouling at the electrode surface; and the “fluidized” extraction format based on electrokinetically as-

sisted mixing and contacting of microbeads in a shape-optimized chamber. A secondary proprietary feature is in the particular layout integrating these components to perform the desired operation of RNA isolation.

Apart from a novel functional capability, advantages of the innovation include reduced or eliminated use of toxic reagents, and operator-independent extraction of RNA.

This work was done by Shivshankar Sundaram, Balabhaskar Prabhakarbandian, Kapil Pant, and Yi Wang of CFD Research

Corp. for Johnson Space Center. Further information is contained in a TSP (see page 1).

In accordance with Public Law 96-517, the contractor has elected to retain title to this invention. Inquiries concerning rights for its commercial use should be addressed to:

CFD Research Corp.

215 Wynn Dr.

Huntsville, AL 35805

Phone No.: (256) 726-4800

E-mail: bio_web@cfdr.com

Refer to MSC-24375-1, volume and number of this NASA Tech Briefs issue, and the page number.

Enabling Microliquid Chromatography by Microbead Packing of Microchannels

Goddard Space Flight Center, Greenbelt, Maryland

The microbead packing is the critical element required in the success of on-chip microfabrication of critical microfluidic components for in-situ analysis and detection of chiral amino acids. In order for microliquid chromatography to occur, there must be a stationary phase medium within the microchannel that interacts with the analytes present within flowing fluid. The stationary phase media are the microbeads packed by the process discussed in this work. The purpose of the microliquid chromatography is to provide a lightweight, low-volume, and low-power element to separate amino acids and their chiral partners efficiently to understand better the origin of life.

In order to densely pack microbeads into the microchannels, a liquid slurry of

microbeads was created. Microbeads were extracted from a commercially available high-performance liquid chromatography column. The silica beads extracted were 5 microns in diameter, and had surface coating of phenyl-hexyl. These microbeads were mixed with a 200-proof ethanol solution to create a microbead slurry with the right viscosity for packing. A microfilter is placed at the outlet via of the microchannel and the slurry is injected, then withdrawn across a filter using modified syringes. After each injection, the channel is flushed with ethanol to enhance packing. This cycle is repeated numerous times to allow for a tightly packed channel of microbeads.

Typical microbead packing occurs in the macroscale into tubes or channels by

using highly pressurized systems. Moreover, these channels are typically long and straight without any turns or curves. On the other hand, this method of microbead packing is completed within a microchannel 75 micrometers in diameter. Moreover, the microbead packing is completed into a serpentine type microchannel, such that it maximizes microchannel length within a microchip. Doing so enhances the interactions of the analytes with the microbeads to separate efficiently amino acids and amino acid enantiomers.

This work was done by Manuel Balvin and Yun Zheng of Goddard Space Flight Center. Further information is contained in a TSP (see page 1). GSC-16514-1

On-Command Force and Torque Impeding Devices (OC-FTID) Using ERF

This technology is applicable as a rehabilitation or exercise device.

NASA's Jet Propulsion Laboratory, Pasadena, California

Various machines have been developed to address the need for countermeasures of bone and muscle deterioration when humans operate over extended time in space. Even though these machines are in use, each of them has many limitations that need to be addressed in an effort to prepare for human missions to distant bodies in the solar system.

An exercise exoskeleton was conceived that performs on-demand resistiv-

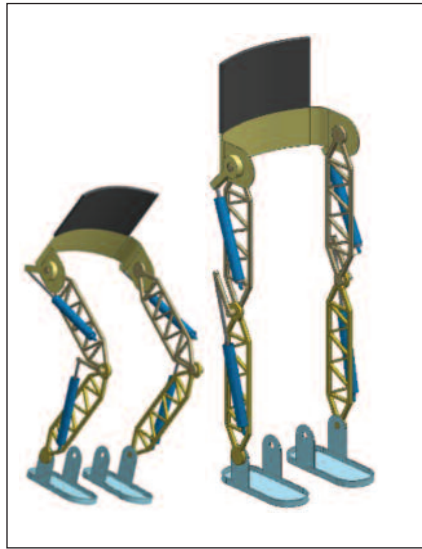
ity by inducing force and torque impedance via ElectroRheological Fluid (ERF). The resistive elements consist of pistons that are moving inside ERF-filled cylinders or a donut-shaped cavity, and the fluid flows through the piston when the piston is moved. Tests of the operation of ERF against load showed the feasibility of this approach.

The inside of the piston consists of parallel electrodes with alternating po-

larity that increase the ERF viscosity when activated. This increase leads to the formation of a virtual valve inside the piston creating impeding force to the piston motion. The cross-sectional area of the piston is mostly hollow to allow low piston resistance to the motion when the electrodes are not activated, and produce high impedance when the electrodes are activated. A balanced volume is created on the two

sides of the piston so that pushing it will only involve fluid flow against the effect of the increased viscosity in the gaps between the electrodes.

The elements are shaped as a cylinder or donut with a piston that is moved inside the internal cavity containing ERF. The elements have a piston inside the cavity with shafts on its two sides. The piston is pushed or pulled inside the chambers and consists of parallel electrodes with opposing polarity wired through one of the shafts. When the electrodes are subjected to electric field, they form a virtual valve causing increased viscosity and impeded flow. Using ERF offers the ability to proportionally (as a function of the voltage) increase the viscosity of the fluid with a very fast reaction time on the order of milliseconds. The feasibility of this approach is straightforward from the nature of ERF materials and preliminary tests made in the lab.



The **Exoskeleton** and the required elements that control the mechanical impedance are shown. The elements are shaped as a cylinder or donut with a piston that is moved inside the internal cavity containing ERF.

ERF properties of high yield stress, low current density, and fast response (less than one millisecond) offer essential characteristics for the construction of the exoskeleton. ERFs can apply very high electrically controlled resistive forces or torque while their size (weight and geometric parameters) can be very small. Their long life and ability to function in a wide temperature range (from -40 to 200 °C) allows for their use in extreme environments. ERFs are also non-abrasive, non-toxic, and nonpolluting (meet health and safety regulations).

The technology is applicable as a compact exercise machine for astronauts' countermeasure of microgravity, an exercise machine for sport, or as a device for rehabilitation of patients with limb issues.

This work was done by Yoseph Bar-Cohen, Mircea Badescu, and Stewart Sherrit of Caltech for NASA's Jet Propulsion Laboratory. Further information is contained in a TSP (see page 1).. NPO-48393



Deployable Fresnel Rings

This antenna technology can be used by first-responders and soldiers requiring cellular range extension or satellite links to handheld devices.

Lyndon B. Johnson Space Center, Houston, Texas

Deployable Fresnel rings (DFRs) significantly enhance the realizable gain of an antenna. This innovation is intended to be used in combination with another antenna element, as the DFR itself acts as a focusing or microwave lens element for a primary antenna. This method is completely passive, and is also completely wireless in that it requires neither a cable, nor a connector from the antenna port of the primary antenna to the DFR.

The technology improves upon the previous NASA technology called a Tri-Sector Deployable Array Antenna in at least three critical aspects. In contrast to the previous technology, this innovation requires no connector, cable, or other physical interface to the primary communication radio or sensor device. The achievable improvement in terms of antenna gain is significantly higher than has been achieved with the previous technology. Also, where previous embodiments of the Tri-Sector antenna have been constructed with combinations of conventional (e.g., printed circuit board) and conductive fabric materials, this innovation is realized using only conductive and non-conductive fabric (i.e., “e-textile”) materials, with the possible exception of a spring-like deployment ring.

Conceptually, a DFR operates by canceling the out-of-phase radiation at a plane by insertion of a conducting ring or rings of a specific size and distance from the source antenna, defined by Fresnel zones. Design of DFRs follow similar procedures to those outlined for conventional Fresnel zone rings.

Gain enhancement using a single ring is verified experimentally and through computational simulation. The experimental test setup involves a microstrip patch antenna that is directly behind a single-ring DFR and is radiating towards a second microstrip patch antenna. The first patch antenna and DFR are shown in Figure 1. At 2.42 GHz, the DFR improves the transmit antenna gain by 8.6 dB, as shown in Figure 2, relative to the wireless link without the DFR. Figure 2 illustrates the relative strength of power

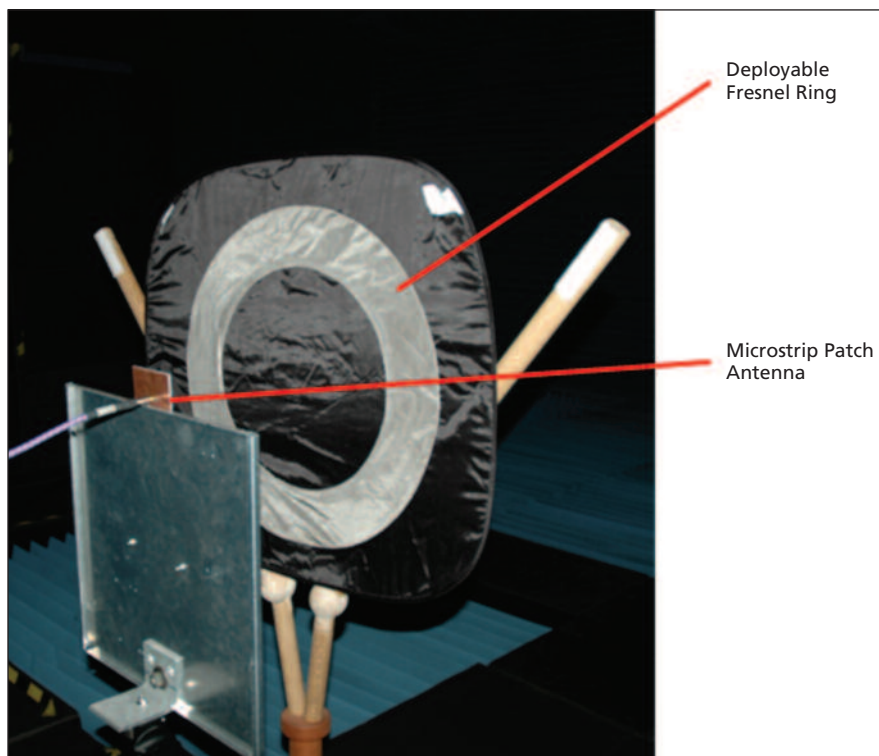


Figure 1. Microstrip Patch Antenna + DFR used in the experimental setup for testing transmitted power enhancement using the DFR.

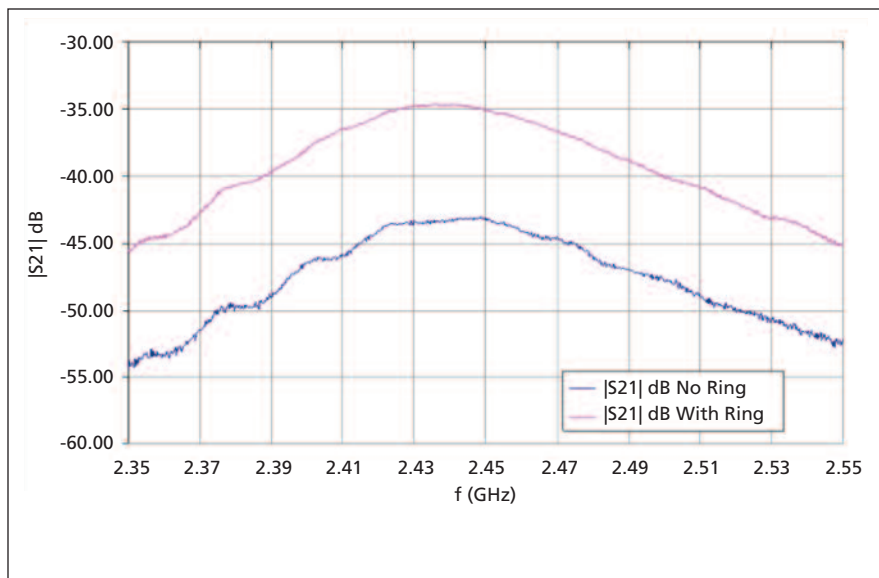


Figure 2. Relative Power received using the DFR and without the DFR.

coupling between the first and second microstrip antennas with and without the DFR. Typically, a DFR is designed for use at a particular frequency; however, testing of a DFR indicated a relatively wide operational bandwidth of approximately 8.2%. Wider bandwidth operation and multi-band operation are anticipated by extending the known art of conventional Fresnel rings to the DFRs.

Increasing the number of rings used to construct a DFR antenna increases

the gain, with the upper bound limited often by the largest practical dimensions that can be tolerated for a given application. The maximum theoretical improvement in gain for a single ring is 9.5 dB. Experimental results are within 0.9 dB of this theoretical value. Adding rings increases gain, and theoretically, improvements of 10 to 13 dB above that of the primary antenna gain can be achieved with two- and three-ring versions.

This work was done by Timothy F. Kennedy, Patrick W. Fink, Andrew W. Chu, and Gregory Y. Lin of Johnson Space Center. Further information is contained in a TSP (see page 1).

This invention has been patented by NASA U.S. Patent No. 8,384,614. Inquiries concerning nonexclusive or exclusive license for its commercial development should be addressed to the Patent Counsel, Johnson Space Center, (281) 483-1003. Refer to MSC-24525-1.

Transition-Edge Hot-Electron Microbolometers for Millimeter and Submillimeter Astrophysics

New instruments promise to expand the investigation of cosmic microwave background radiation and its polarization to get better insight into the evolution of the universe.

Goddard Space Flight Center, Greenbelt, Maryland

The millimeter and the submillimeter wavelengths of the electromagnetic spectrum hold a wealth of information about the evolution of the universe. In particular, cosmic microwave background (CMB) radiation and its polarization carry the oldest information in the universe, and provide the best test of the inflationary paradigm available to astronomy today. Detecting gravity waves through their imprint on the CMB polarization would have extraordinary repercussions for cosmology and physics.

A transition-edge hot-electron microbolometer (THM) consists of a superconducting bilayer transition-edge sensor (TES) with a thin-film absorber. Unlike traditional monolithic bolometers that make use of micromachined structures, the THM employs the decoupling between electrons and phonons at millikelvin temperatures to provide thermal isolation. The devices are fabricated photolithographically and are easily in-

tegrated with antennas via microstrip transmission lines, and with SQUID (superconducting quantum interference device) readouts. The small volume of the absorber and TES produces a short thermal time constant that facilitates rapid sky scanning.

The THM consists of a thin-film metal absorber overlapping a superconducting TES. The absorber forms the termination of a superconducting microstripline that carries RF power from an antenna. The purpose of forming a separate absorber and TES is to allow flexibility in the optimization of the two components. In particular, the absorbing film's impedance can be chosen to match the antenna, while the TES impedance can be chosen to match to the readout SQUID amplifier. This scheme combines the advantages of the TES with the advantages of planar millimeter-wave transmission line circuits.

Antenna-coupling to the detectors via planar transmission lines allows the de-

tector dimensions to be much smaller than a wavelength, so the technique can be extended across the entire microwave, millimeter, and submillimeter wavelength ranges. The circuits are fabricated using standard microlithographic techniques and are compatible with uniform, large array formats. Unlike traditional monolithic bolometers that make use of micromachined structures, the THM employs the decoupling between electrons and phonons at millikelvin temperatures to provide thermal isolation. There is no fragile membrane in the structure for thermal isolation, which improves the fabrication yield.

This work was done by Wen-Ting Hsieh, Thomas Stevenson, Kongpop U-yen, and Edward Wollack of Goddard Space Flight Center; and Emily Barrentine of the University of Wisconsin at Madison. Further information is contained in a TSP (see page 1). GSC-16656-1



Spacecraft Trajectory Analysis and Mission Planning Simulation (STAMPS) Software

STAMPS simulates either three- or six-degree-of-freedom cases for all spacecraft flight phases using translated HAL flight software or generic GN&C models. Single or multiple trajectories can be simulated for use in optimization and dispersion analysis. It includes math models for the vehicle and environment, and currently features a “C” version of shuttle onboard flight software. The STAMPS software is used for mission planning and analysis within ascent/descent, rendezvous, proximity operations, and navigation flight design areas.

This work was done by Nancy Puckett, Kris Pettinger, John Hallstrom, Dana Brownfield, Eric Blinn, Frank Williams, Kelli Wiuff, Steve McCarty, Daniel Ramirez, Nicole Lamotte, and Tuan Vu of United Space Alliance for Johnson Space Center. For further information, contact the JSC Innovation Partnerships Office at (281) 483-3809. MSC-24958-1

Cross Support Transfer Service (CSTS) Framework Library

Within the Consultative Committee for Space Data Systems (CCSDS), there is an effort to standardize data transfer between ground stations and control centers. CCSDS plans to publish a collection of transfer services that will each address the transfer of a particular type of data (e.g., tracking data). These services will be called Cross Support Transfer Services (CSTSs). All of these services will make use of a common foundation that is called the CSTS Framework. This library implements the User side of the CSTS Framework. “User side” means that the library performs the role that is typically expected of the control center.

This library was developed in support of the Goddard Data Standards program. This technology could be applicable for control centers, and possibly for use in control center simulators needed to test ground station capabilities. The main advantages of this implementation are its flexibility and simplicity. It provides the framework capabilities, while allowing the library user to provide a

wrapper that adapts the library to any particular environment.

The main purpose of this implementation was to support the inter-operability testing required by CCSDS. In addition, it is likely that the implementation will be useful within the Goddard mission community (for use in control centers).

This work was done by Timothy Ray of Goddard Space Flight Center. Further information is contained in a TSP (see page 1). GSC-16068-1

Arbitrary Shape Deformation in CFD Design

Sculptor[®] is a commercially available software tool, based on an Arbitrary Shape Design (ASD), which allows the user to perform shape optimization for computational fluid dynamics (CFD) design. The developed software tool provides important advances in the state-of-the-art of automatic CFD shape deformations and optimization software. CFD is an analysis tool that is used by engineering designers to help gain a greater understanding of the fluid flow phenomena involved in the components being designed. The next step in the engineering design process is to then modify, the design to improve the components’ performance. This step has traditionally been performed manually via trial and error. Two major problems that have, in the past, hindered the development of an automated CFD shape optimization are (1) inadequate shape parameterization algorithms, and (2) inadequate algorithms for CFD grid modification.

The ASD that has been developed as part of the *Sculptor*[®] software tool is a major advancement in solving these two issues. First, the ASD allows the CFD designer to freely create his own shape parameters, thereby eliminating the restriction of only being able to use the CAD model parameters. Then, the software performs a smooth volumetric deformation, which eliminates the extremely costly process of having to remesh the grid for every shape change (which is how this process had previously been achieved). *Sculptor*[®] can be used to optimize shapes for aerodynamic and structural design of spacecraft, aircraft, watercraft, ducts, and other objects that affect

and are affected by flows of fluids and heat. *Sculptor*[®] makes it possible to perform, in real time, a design change that would manually take hours or days if remeshing were needed.

This program was written by Mark Landon and Ernest Perry of Optimal Solutions Software, LLC for Stennis Space Center. For more information, contact Optimal Solutions at 208-521-4660. Refer to SSC-00290.

Range Safety Flight Elevation Limit Calculation Software

This program was developed to fill a need within the Wallops Flight Facility workflow for automation of the development of vertical plan limit lines used by flight safety officers during the conduct of expendable launch vehicle missions.

Vertical plane present-position-based destruct lines have been used by range safety organizations at numerous launch ranges to mitigate launch vehicle risks during the early phase of flight. Various ranges have implemented data submittal and processing workflows to develop these destruct lines. As such, there is significant prior art in this field. The EILimits program was developed at NASA’s Wallops Flight Facility to automate the process for developing vertical plane limit lines using current computing technologies.

The EILimits program is used to configure launch-phase range safety flight control lines for guided missiles. The name of the program derives itself from the fundamental quantity that is computed — flight elevation limits. The user specifies the extent and resolution of a grid in the vertical plane oriented along the launch azimuth. At each grid point, the program computes the maximum velocity vector flight elevation that can be permitted without endangering a specified back-range location. Vertical plane x-y limit lines that can be utilized on a present position display are derived from the flight elevation limit data by numerically propagating ‘streamlines’ through the grid.

The failure turn and debris propagation simulation technique used by the application is common to all of its analysis options. A simulation is initialized at a vertical plane grid point chosen by the program. A powered flight failure turn

is then propagated in the plane for the duration of the so-called RSO reaction time. At the end of the turn, a delta-velocity is imparted, and a ballistic trajectory is propagated to impact.

While the program possesses capability for powered flight failure turn mod-

eling, it does not require extensive user inputs of vehicle characteristics (e.g., thrust and aerodynamic data), nor does it require reams of turn data after the traditional fashion of the Air Force ranges. The program requires a nominal trajectory table (time, altitude,

range, velocity, and flight elevation) and makes heavy use of it to initialize and model a failure turn.

This work was done by Raymond J. Lanzi of Goddard Space Flight Center. Further information is contained in a TSP (see page 1). GSC-16692-1



Frequency-Modulated, Continuous-Wave Laser Ranging Using Photon-Counting Detectors

NASA's Jet Propulsion Laboratory, Pasadena, California

Optical ranging is a problem of estimating the round-trip flight time of a phase- or amplitude-modulated optical beam that reflects off of a target. Frequency-modulated, continuous-wave (FMCW) ranging systems obtain this estimate by performing an interferometric measurement between a local frequency-modulated laser beam and a delayed copy returning from the target. The range estimate is formed by mixing the target-return field with the local reference field on a beamsplitter and detecting the resultant beat modulation. In conventional FMCW ranging, the source modulation is linear in instantaneous frequency, the reference-arm field has many more photons than the target-return field, and the time-of-flight estimate is generated by balanced difference-detection of the beamsplitter output, followed by a frequency-domain peak search.

This work focused on determining the maximum-likelihood (ML) estimation algorithm when continuous-time photon-counting detectors are used. It is founded on a rigorous statistical characterization of the (random) photoelectron emission times as a function of the incident optical field, including the deleterious effects caused by dark current and dead time. These statistics enable derivation of the Cramér-Rao lower bound (CRB) on the accuracy of FMCW ranging, and derivation of the ML estimator, whose performance approaches this bound at high photon flux.

The estimation algorithm was developed, and its optimality properties were shown in simulation. Experimental data show that it performs better than the conventional estimation algorithms used. The demonstrated improvement is a factor of 1.414 over frequency-domain-based estimation.

If the target interrogating photons and the local reference field photons are costed equally, the optimal allocation of photons between these two arms is to have them equally distributed. This is different than the state of the art, in which the local field is stronger than the target return. The optimal processing of the photocurrent processes at the outputs of the two detectors is to perform log-matched filtering followed by a summation and peak detection. This implies that neither difference detection, nor Fourier-domain peak detection, which are the staples of the state-of-the-art systems, is optimal when a weak local oscillator is employed.

This work was done by Baris I. Erkmen of Caltech, and Zeb W. Barber and Jason Dahl of Montana State University for NASA's Jet Propulsion Laboratory. For more information, contact iaoffice@jpl.nasa.gov. NPO-48866

Calculation of Operations Efficiency Factors for Mars Surface Missions

Several modeling methods are examined.

NASA's Jet Propulsion Laboratory, Pasadena, California

For planning of Mars surface missions, to be operated on a sol-by-sol basis by a team on Earth (where a "sol" is a Martian day), activities are described in terms of "sol types" that are strung together to build a surface mission scenario. Some sol types require ground decisions based on a previous sol's results to feed into the activity planning ("ground in the loop"), while others do not. Due to the differences in duration between Earth days and Mars sols, for a given Mars local solar time, the corresponding Earth time "walks" relative to the corresponding times on the prior sol/day. In particular, even if a communication window has a fixed Mars local solar time, the

Earth time for that window will be approximately 40 minutes later each succeeding day. Further complexity is added for non-Mars synchronous communication relay assets, and when there are multiple control centers in different Earth time zones.

The solution is the development of "ops efficiency factors" that reflect the efficiency of a given operations configuration (how many and location of control centers, types of communication windows, synchronous or non-synchronous nature of relay assets, sol types, more-or-less sustainable operations schedule choices) against a theoretical "optimal" operations configuration for the mission being studied.

These factors are then incorporated into scenario models in order to determine the surface duration (and therefore minimum spacecraft surface lifetime) required to fulfill scenario objectives. The resulting model is used to perform "what-if" analyses for variations in scenario objectives. The ops efficiency factor is the ratio of the figure of merit for a given operations factor to the figure of merit for the theoretical optimal configuration.

The current implementation is a pair of models in Excel. The first represents a ground operations schedule for 500 sols in each operations configuration for the mission being studied (500 sols was chosen as being a long enough time to

capture variations in relay asset interactions, Earth/Mars time phasing, and seasonal variations in holidays). This model is used to estimate the ops efficiency factor for each operations configuration.

The second model in a separate Excel spreadsheet is a scenario model, which uses the sol types to rack up the total number of “scenario sols” for that scenario (in other words, the ideal number of sols it would take to perform the scenario objectives). Then, the number of sols requiring ground in the loop is cal-

culated based on the soil types contained in the given scenario. Next, the scenario contains a description of what sequence of operations configurations is used, for how many days each, and this is used with the corresponding ops efficiency factors for each configuration to calculate the “ops duration” corresponding to that scenario. Finally, a margin is applied to determine the minimum surface lifetime required for that scenario.

Typically, this level of analysis has not been performed until much later in the

mission, and has not been able to influence mission design. Further, the notion of moving to sustainable operations during Prime Mission — and the effect that that move would have on surface mission productivity and mission objective choices — has not been encountered until the most recent rover missions (MSL and Mars 2018).

This work was done by Sharon L. Layback of Caltech for NASA’s Jet Propulsion Laboratory. Further information is contained in a TSP (see page 1). NPO-48262

GPU Lossless Hyperspectral Data Compression System

NASA’s Jet Propulsion Laboratory, Pasadena, California

Hyperspectral imaging systems onboard aircraft or spacecraft can acquire large amounts of data, putting a strain on limited downlink and storage resources. Onboard data compression can mitigate this problem but may require a system capable of a high throughput. In order to achieve a high throughput with a software compressor, a graphics processing unit (GPU) implementation of a compressor was developed targeting the current state-of-the-art GPUs from NVIDIA®.

The implementation is based on the fast lossless (FL) compression algorithm reported in “Fast Lossless Compression

of Multispectral-Image Data” (NPO-42517), *NASA Tech Briefs*, Vol. 30, No. 8 (August 2006), page 26, which operates on hyperspectral data and achieves excellent compression performance while having low complexity. The FL compressor uses an adaptive filtering method and achieves state-of-the-art performance in both compression effectiveness and low complexity. The new Consultative Committee for Space Data Systems (CCSDS) Standard for Lossless Multispectral & Hyperspectral image compression (CCSDS 123) is based on the FL compressor. The software makes use of the highly-parallel processing capa-

bility of GPUs to achieve a throughput at least six times higher than that of a software implementation running on a single-core CPU. This implementation provides a practical real-time solution for compression of data from airborne hyperspectral instruments.

This work was done by Nazeeh I. Aranki, Didier Keymeulen, Aaron B. Kieby, and Matthew A. Klimesh of Caltech for NASA’s Jet Propulsion Laboratory. For more information, contact iaoffice@jpl.nasa.gov.

The software used in this innovation is available for commercial licensing. Please contact Dan Broderick at Daniel.F.Broderick@jpl.nasa.gov. Refer to NPO-48571.

Robust, Optimal Subsonic Airfoil Shapes

Ames Research Center, Moffett Field, California

A method has been developed to create an airfoil robust enough to operate satisfactorily in different environments. This method determines a robust, optimal, subsonic airfoil shape, beginning with an arbitrary initial airfoil shape, and imposes the necessary constraints on the design. Also, this method is flexible and extendible to a larger class of requirements and changes in constraints imposed.

In one embodiment, process steps include providing a specification of a desired pressure value at each of a sequence of selected locations on the surface of a turbine airfoil; providing an initial airfoil shape; providing a statement of at least one constraint to which a final airfoil shape must conform; using computational fluid dynamics (CFD) to estimate a pressure value at each of the

selected perimeter locations for the initial airfoil shape; using CFD to determine the pressure distribution for the airfoil shapes that are small perturbations to the initial airfoil shape; and using an estimation method, such as a neural network, a support vector machine, or a combination thereof, to construct a response surface that models the pressure distribution as a function of the airfoil shape using the CFD data. Other process steps include using an optimization algorithm to search the response surface for the airfoil shape having the required pressure distribution, and providing at least one of an alphanumeric description and a graphical description of the modified airfoil shape.

Constraints may be drawn from the following group, or may be one or more other suitable constraints: vortex shed-

ding strength from the trailing edge of the airfoil is no greater than a selected threshold value; a difference between any resonant frequency of the airfoil and the vortex shedding frequency is at least equal to a threshold frequency difference; mass of the airfoil is no larger than a threshold mass value; and pressure value at each of a sequence of selected locations along the surface of the airfoil differs from a corresponding reference pressure value by no more than a threshold pressure difference value.

This work was done by Man Mohan Rai of Ames Research Center. Further information is contained in a TSP (see page 1).

Inquiries concerning rights for the commercial use of this invention should be addressed to the Ames Technology Partnerships Division at 1-855-NASA-BIZ (1-855-6272-249). Refer to ARC-14586-2

▶ Protograph-Based Raptor-Like Codes

The proposed codes have the advantage of low-complexity encoder and decoder implementation.

NASA's Jet Propulsion Laboratory, Pasadena, California

Theoretical analysis has long indicated that feedback improves the error exponent but not the capacity of point-to-point memoryless channels. The analytic and empirical results indicate that at short blocklength regime, practical rate-compatible punctured convolutional (RCPC) codes achieve low latency with the use of noiseless feedback. In 3GPP, standard rate-compatible turbo codes (RCPT) did not outperform the convolutional codes in the short blocklength regime. The reason is the convolutional codes for low number of states can be decoded optimally using Viterbi decoder. Despite excellent performance of convolutional codes at very short blocklengths, the strength of convolutional codes does not scale with the blocklength for a fixed number of states in its trellis.

Protograph-based (PB) Raptor-like codes can provide good performance in an incremental redundancy scheme with noiseless feedback over an additive white Gaussian noise channel. Additionally, these codes are also desirable

for other applications where there is a need for simple generation of various code rates.

The proposed codes are based on protograph construction and they represent a novel contribution. In the original Raptor code, the redundant bit generation is based on a random selection of precoded bits that are produced from an unstructured LDPC (Low Density Parity Check) code. These redundant bits are selected based on some optimized distribution. Due to the nature of random selection, the original Raptor code required some additional information to be transmitted to the receiver in order to enable the decoding process. In the proposed codes, the redundant bits are generated based to optimized protograph structure with degree-1 nodes. Thus they do not need any additional information to be transmitted to the receiver. The proposed codes with protograph-based structure have the advantage of low-complexity encoder and decoder implementation. The proposed codes were designed for short block sizes, but a similar construction

method can be applied to longer block lengths for other applications.

Hybrid ARQ (hybrid automatic repeat request — HARQ) is an error control method. In standard ARQ error detection, symbols such as cyclic redundancy check (CRC) are added to the information data. In HARQ, forward error correction code such as LDPC code symbols are also added to the existing error detection symbols, such that small random errors are corrected without retransmission, and major errors are corrected via a request for retransmission. The hybrid scheme performs better than standard ARQ in poor signal conditions. The proposed protograph-based Raptor-like codes can be used with HARQ.

This work was done by Dariush Divsalar of Caltech; and Tsung-Yi Chen, Jiadong Wang, and Richard D. Wesel of UCLA for NASA's Jet Propulsion Laboratory. For more information, contact iaoffice@jpl.nasa.gov.

The software used in this innovation is available for commercial licensing. Please contact Dan Broderick at Daniel.F.Broderick@jpl.nasa.gov. Refer to NPO-48128.

▶ Fuzzy Neuron: Method and Hardware Realization

Simple and effective learning functions and adaptive elements can be placed into small hardware systems to include instruments for space, bioimplantable devices, and stochastic observers.

John H. Glenn Research Center, Cleveland, Ohio

This innovation represents a method by which single-to-multi-input, single-to-many-output system transfer functions can be estimated from input/output data sets. This innovation can be run in the background while a system is operating under other means (e.g., through human operator effort), or may be utilized offline using data sets created from observations of the estimated system. It utilizes a set of fuzzy membership functions spanning the input space for each input variable. Linear combiners associated with combinations of input membership functions are used to create the output(s) of the estimator. Coefficients are adjusted online through the use of learning algorithms.

This innovation has been demonstrated to be capable of creating usable

models that can effect any number of complex transfer functions such as a continuous exclusive OR function, time domain (slew rate) filter, automatic gain controller, non-linear algebraic function calculator, and more. This innovation was created specifically for embedment within microcontrollers, allowing for simple and effective placement of learning functions and adaptive elements into small hardware systems to include instruments for space, bioimplantable devices, stochastic observers, etc.

Small spaceflight (and other) instruments have been confined to simple systems utilizing microcontrollers and a microcontroller core. Since most learning algorithms typically reside in larger computational frames and are rather complex (neural nets, for example), a

simpler solution to self-learning, auto-adaptive systems would be attractive for smaller embodiments. Fuzzy logic systems lend themselves well to microcontrollers, but adaptive fuzzy systems also require a good deal of computational power. Thus, the simpler components of both fuzzy systems (input membership functions) and the back error propagation neural net (the linear combiner) were selected and fused into a simple two-layer system that can be easily embedded into common microcontrollers.

The training method used is an LMS (least mean square) algorithm based on a modification to the Widrow-Hoff learning algorithm. Coefficients and constants for each linear combiner were initialized to random values. Training data from observations of a user's

input(s) to a system and the resultant output(s) in real time or a posteriori, or from software-generated data sets, were presented to the system, which generated outputs. Once a system is learned, the coefficients and constants can be

frozen and the algorithm embedded in an application.

This work was done by Michael J. Krasowski and Norman F. Prokop of Glenn Research Center. Further information is contained in a TSP (see page 1).

Inquiries concerning rights for the commercial use of this invention should be addressed to NASA Glenn Research Center, Innovative Partnerships Office, Attn: Steven Fedor, Mail Stop 4-8, 21000 Brookpark Road, Cleveland, Ohio 44135. Refer to LEW-18887-1.

➤ **Kalman Filter Input Processor for Boresight Calibration**

The new software brings this technology to the industrial level.

NASA's Jet Propulsion Laboratory, Pasadena, California

Ka-band ranging provides the phase center (PC) to phase center range, which needs to be converted to the center of mass (CM) to center of mass range. Nominally, both PC and CM lie on the line connecting the spacecraft GRAIL A and GRAIL B. In this case, the conversion should be done simply by adding the CM-to-PC distance L to the measured range for both spacecraft. However, due to various technical reasons, such as displacement of the true CM from its nominal position in the SRF, or spacecraft attitude fluctuations, the PC and CM define a unit vector that may be different from the nominal line of sight. The objectives of the software are to determine the actual line of sight direction for each spacecraft and correct the previously recorded range data, and to provide instructions for how to ma-

neuver each spacecraft to make necessary attitude corrections.

While elements of this approach have been used for the boresight calibration in the GRACE project, the new software brings this technology to the industrial level. It is now fully documented and can be used by people other than its developers. This innovation provides graphic outputs and log files that are critical for quick analysis and troubleshooting. In addition to the line of sight direction, the software allows one to evaluate the CM-PC base length, which is important when the PM location is subject to variations (e.g., due to fuel depletion).

This software is implemented in Python and offers excellent cross-platform porting possibilities. It is very versatile, and may be applied under various circumstances and for other related pur-

poses. This innovation is capable of combining the input data from several calibration maneuvers, evaluating individual range biases, and compressing the time stamps. It uses Lagrange interpolation for the orbit data, and a unique quaternion-interpolating algorithm for interpolating the attitude data. As a result, data files with different data rates and independent time stamps can be handled together.

This work was done by Dmitry V. Strelkov, Gerhard L. Kruizinga, Meegyeong Paik, Dah-Ning Yuan, and Sami W. Asmar of Caltech for NASA's Jet Propulsion Laboratory. For more information, please contact Brian Morrison at Brian.A.Morrison@jpl.nasa.gov.

This software is available for commercial licensing. Please contact Dan Broderick at Daniel.F.Broderick@jpl.nasa.gov. Refer to NPO-48479.

➤ **Organizing Compression of Hyperspectral Imagery to Allow Efficient Parallel Decompression**

Higher compression factors can be attained.

NASA's Jet Propulsion Laboratory, Pasadena, California

A family of schemes has been devised for organizing the output of an algorithm for predictive data compression of hyperspectral imagery so as to allow efficient parallelization in both the compressor and decompressor. In these schemes, the compressor performs a number of iterations, during each of which a portion of the data is compressed via parallel threads operating on independent portions of the data. The general idea is that for each iteration it is predetermined how much compressed data will be produced from each thread.

A simple version of this technique is applicable when the image is divided into "pieces" that are compressed inde-

pendently. As an example, for a compressor that does not make use of inter-band correlation, a piece could be defined to be an individual spectral band, or a fixed number of bands. In the technique, the compressed output for a piece is comprised of multiple "chunks." The concatenated chunks for a given piece form the compressed output for the piece. Most of the compressed image is produced in multiple iterations, where during a given iteration, one chunk is produced for each piece. Prior to the start of an iteration, chunk sizes are calculated for each piece. The chunks can be produced or decompressed in parallel. It is noted that it is not specified how

much of the image data will go into a chunk, and in fact a chunk may contain incomplete portions of encoded samples (at the chunk's start or end). The compressor iterates the process of deciding on chunk sizes and producing chunks for each piece of the requested size, until compression of each piece is almost finished. At that point, the remainder of the pieces is compressed serially without a target chunk size.

Typically, the chunk size calculation should seek to balance the progress through each piece, i.e., to leave equal numbers of samples remaining in each piece; a suggested procedure has this aim. A key requirement on the chunk

size calculation is that reasonable chunk sizes must be decided on based only on information from the compressed data available at a given point in the process. Similarly, from previous data, it must be possible to evaluate when to switch from the parallel chunk compression to the

serial process that completes compression of each piece.

A more general technique accommodates pieces that are not compressed independently, allowing compressors such as the Fast Lossless (FL) to more fully exploit dependencies between spectral

bands, which generally allows a higher compression factor to be achieved.

This work was done by Matthew A. Klimesh and Aaron B. Kiely of Caltech for NASA's Jet Propulsion Laboratory. Further information is contained in a TSP (see page 1). NPO-48521

Temperature Dependences of Mechanisms Responsible for the Water-Vapor Continuum Absorption

Results can be used to develop better empirical models.

Goddard Space Flight Center, Greenbelt, Maryland

The water-vapor continuum absorption plays an important role in the radiative balance in the Earth's atmosphere. It has been experimentally shown that for ambient atmospheric conditions, the continuum absorption scales quadratically with the H₂O number density and has a strong, negative temperature dependence (T dependence). Over the years, there have been three different theoretical mechanisms postulated: far-wings of allowed transition lines, water dimers, and collision-induced absorption. The first mechanism proposed was the accumulation of absorptions from the far-wings of the strong allowed transition lines. Later, absorption by water dimers was proposed, and this mechanism provides a qualitative explanation for the continuum characters mentioned above. Despite the improvements in experimental data, at present there is no consensus on which mechanism is primarily responsible for the continuum absorption.

Because all three mechanisms scale as the square of the H₂O monomer number density, one way to discriminate between the mechanisms is by their T dependences. This work involved a

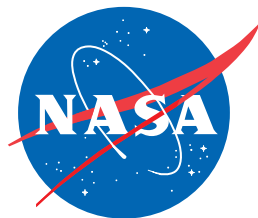
detailed study of the T dependence of the continuum absorption based on the far-wing theory. Because the calculated absorption coefficients, especially their T dependences, match the new NIST measurements very well, one can conclude that in the 800 to 1,150 cm⁻¹ region, contributions from far-wings of allowed H₂O lines are the dominant source responsible for the continuum.

Although all three mechanisms have a negative T dependence, their T dependences would be characterized by individual features. To analyze the characteristics of the latter will enable one to assess their roles with more certainty. The dimer spectra exhibit a very strong negative T dependence, the far-wing theory exhibits a moderately strong negative one, and the collision-induced absorption has a weak and mainly negative T dependence. In addition, these three have quite different T dependence patterns, i.e., the strength of its T dependence varies differently as the frequency of interest varies.

The far-wing theory exhibits the most complex T dependence pattern and it could vary significantly as the frequency

of interest varies. On the other hand, the collision-induced absorption spectra exhibit a systematic T dependence with frequency. Finally, the pattern of the T dependence of the dimer absorption is rather simpler. By comparing theoretical calculations from the far-wing theory with the most recent and accurate experimental data at different temperatures ranging from 310.8 to 363.6 K in the infrared windows, it was found that theoretical results agree very well with measurements in the 800 to 1,200 cm⁻¹ region. Meanwhile, the new measurements show that at room temperature, the continuum data are in reasonable agreement with the widely used semi-empirical MT_CKD continuum model, but at higher temperatures, the MT_CKD model provides very low values, up to 50% less than those experimentally measured. This indicates that the T dependence exhibited in the current MT_CKD model is not correct, and this model has to be modified.

This work was done by Qiancheng Ma of Goddard Space Flight Center. Further information is contained in a TSP (see page 1). GSC-16075-1



National Aeronautics and
Space Administration